AGU ADVANCING EARTH AND SPACE SCIENCES

Geophysical Research Letters

RESEARCH LETTER
10.1029/2024GL108924

Asymmetric Efficacies Between Warm and Cold Pacific Meridional Modes in Inducing ENSO

Xumin Li[1,2,3], Jin-Yi Yu[2], Ruiqiang Ding[1], Jianyu Hu[4], and Peng-Fei Tuo[5]

[1]Key Laboratory of Environmental Change and Natural Disasters of Chinese Ministry of Education, Beijing Normal University, Beijing, China, [2]Department of Earth System Science, University of California, Irvine, CA, USA, [3]Key Laboratory of Meteorological Disaster of Ministry of Education (KLME), Nanjing University of Information Science and Technology, Nanjing, China, [4]State Key Laboratory of Marine Environmental Science, College of Ocean and Earth Sciences, Xiamen University, Xiamen, China, [5]Shenzhen International Graduate School, Institute for Ocean Engineering, Tsinghua University, Shenzhen, China

Key Points:

- The cold phase of Pacific Meridional Mode (PMM) has a higher efficacy in inducing following La Niña than warm PMM in inducing El Niño
- Disparate efficacies arise from distinct origins of the two PMMs and their varied competition with tropical discharge-recharge processes
- Cold/warm PMM, induced by a previous La Niña/El Niño, encounters weak/strong competition from recharge/discharge in triggering El Niño-Southern Oscillation

Supporting Information:

Supporting Information may be found in the online version of this article.

Correspondence to:

J.-Y. Yu,
jyyu@uci.edu

Citation:

Li, X., Yu, J.-Y., Ding, R., Hu, J., & Tuo, P.-F. (2024). Asymmetric efficacies between warm and cold Pacific meridional modes in inducing ENSO. *Geophysical Research Letters*, *51*, e2024GL108924. https://doi.org/10.1029/2024GL108924

Received 21 FEB 2024
Accepted 28 APR 2024

Abstract

This study investigates boreal spring events of Pacific Meridional Mode (PMM) from 1950 to 2022, revealing that cold PMM is more effective in triggering subsequent La Niña compared to warm PMM's induction of following El Niño. This asymmetry stems from the varying origins and sub-efficacies of PMM groups. The cold PMM is primarily initiated by pre-existing La Niña, while the warm PMM is comparably activated by pre-existing El Niño and internal atmospheric dynamics. PMMs initiated by pre-existing El Niño or La Niña play a crucial role in determining the efficacies of PMMs in triggering subsequent El Niño-Southern Oscillation (ENSO). The strong discharge of pre-existing El Niño hampers warm PMM's induction of subsequent El Niño, whereas weak recharge from pre-existing La Niña enhances the efficacy of cold PMM in inducing subsequent La Niña. Comprehending not only the PMM phase but also its origin is crucial for ENSO research and prediction.

Plain Language Summary

This study investigated the efficacies of warm and cold Pacific Meridional Mode (PMM) events in triggering El Niño and La Niña events from 1950 to 2022. Contrary to previous beliefs, the research concludes that cold PMM are more adept at inducing La Niña. The varying efficacies are linked to the fact that cold PMM are primarily initiated by preceding La Niña occurrences, while warm PMM are comparably activated by the subtropical atmospheric internal dynamics and previous El Niño events. Due to the weaker ocean heat content recharge associated with pre-existing La Niña compared to the discharge associated with pre-existing El Niño, La Niña-induced cold PMM encounters less competition from tropical discharge-recharge processes in inducing a subsequent La Niña. In contrast, El Niño-activated warm PMM faces stronger competition in inducing an El Niño. Consequently, the distinct origins of cold and warm PMM phases, along with their competition with tropical discharge-recharge processes, contribute to their respective efficacies in inducing El Niño and La Niña.

1. Introduction

The Pacific Meridional Mode (PMM) originating from the North Pacific Ocean (Chiang & Vimont, 2004) has been recognized as an effective precursor to El Niño-Southern Oscillation (ENSO) events (Wang et al., 2017; Yang et al., 2018), providing the potential for predicting ENSO occurrence up to nine months in advance (Chang et al., 2007; Larson and Kirtman, 2014). The PMM typically reaches its peak during boreal spring (Meng & Li, 2023). Its warm and cold phases are characterized by respective warm and cold sea surface temperature anomalies (SSTAs) extending from Baja California toward the central equatorial region, accompanied by anomalous southwesterly and northeasterly winds overhead. Warm PMM usually precede subsequent El Niño, while cold PMM lead to La Niña through either a seasonal footprinting mechanism (Vimont et al., 2001, 2003), gradually propagating SSTAs and surface wind anomalies from the subtropic Pacific into the tropics, or a trade wind charge mechanism (Anderson et al., 2013), transporting subsurface water into the tropics.

The PMM is considered critically important for the formation of Central Pacific (CP) ENSO (Yu et al., 2010; Yu & Kim, 2011) and multi-year ENSO (Ding et al., 2022; Fang & Yu, 2020a, 2020b). The PMM plays a crucial role in promoting the development of CP ENSO due to its northeast-southwest spatial orientation, which is particularly effective in generating SSTAs toward the central equatorial Pacific (Yu et al., 2010; Yu & Kim, 2011). CP ENSO, in turn, can activate another PMM by triggering atmospheric wavetrains that propagate from the tropical to subtropical North Pacific (Fang & Yu, 2020a, 2020b). The ENSO-induced PMM subsequently influences the occurrence of consecutive ENSO of the same phase in the second year, thereby promoting the formation of multi-year ENSO.

Recent research has highlighted the differing capacities of warm and cold PMM phases in triggering ENSO (Fan et al., 2021; Thomas & Vimont, 2016; Zheng et al., 2021). These studies assessed PMM capabilities by examining SSTA intensity associated with subsequent ENSO induced by PMM. They found that El Niños triggered by warm PMM are more intense than La Niñas triggered by cold PMM. This intensity asymmetry is attributed to stronger summer deep convection during warm PMM, resulting in more pronounced tropical westerly anomalies than during cold PMM. Consequently, warm PMM benefits from a more potent Wind-Evaporation-SST (WES; Xie & Philander, 1994) feedback, enabling it to induce stronger El Niño compared to cold PMM's induction capability for La Niña. However, higher intensity doesn't necessarily imply that warm PMM has a greater likelihood of inducing El Niño compared to cold PMM inducing La Niña. In this study, we examine PMM efficiency by considering proportions of warm and cold PMM leading to corresponding El Niño and La Niña, regardless of magnitudes. To avoid confusion with previous studies, we use "efficacy" to denote the percentage-related ability, forming the central focus of our investigation.

Another aspect overlooked in prior research is the competition between PMM and the tropical discharge-recharge process in shaping ENSO occurrences. It is widely recognized that during an ENSO's lifecycle, the tropical Pacific undergoes significant discharge and recharge of subsurface ocean heat content (OHC) to transition between ENSO phases (Jin, 1997). Consequently, El Niño (La Niña) typically lead to a discharged (recharged) OHC state in the tropical Pacific, favoring the development of a La Niña (El Niño) condition in the subsequent year. When PMM extends into the tropical Pacific, its ability to trigger an ENSO might be influenced by the independent operation of the discharge-recharge process. This potential competition is another central focus of our current investigation.

2. Methods

2.1. Definitions of Indices and ENSO and PMM Events

The PMM index is obtained online (https://www.aos.wisc.edu/~dvimont/MModes/Data.html) via Maximum Covariance Analysis (MCA) on SST and surface wind anomalies in the tropical Pacific (21°S–32°N, 175°E–95°W), post-exclusion of Cold Tongue Index regressions (Chiang & Vimont, 2004). Post MCA analysis produces two indices: the principal component for the leading MCA mode (PC1) in SSTAs, termed PMM SST index, and the PC1 for wind anomalies, called PMM Wind index. This study primarily used the commonly employed PMM SST index as the PMM index. Additionally, we incorporate the PMM Wind index and another newly proposed PMM area-averaged index (SSTAs over 115°–155°W, 10°–30°N) (Fan et al., 2023a, 2023b; Richter et al., 2022) for result verification. A warm (cold) PMM event is identified when the PMM index during the boreal spring (March-April-May, MAM) is greater (less) than or equal to 0.5 (−0.5) standard deviation. In the analysis period from 1950 to 2022, a total of 24 warm PMM events and 21 cold PMM events were identified (Table S1 in Supporting Information S1).

El Niño (La Niña) events are identified when the Niño3.4 index (SSTAs averaged between 5°S–5°N and 170°–120°W) during November-December-January (NDJ; in which the Niño3.4 variance is biggest) exceeds 0.5 (falls below −0.5) standard deviation. All other conditions are recognized as neutral state. The Niño3.4 index is also utilized to quantify the strength of ENSO events.

A two-tailed Student's *t*-test is used to examine the statistical significance of composite analysis results.

2.2. Quantification of PMM Efficacy in Inducing ENSO

The efficacy of warm or cold PMM in inducing ENSO is evaluated by the ratio of the number of El Niño (La Niña) occurrences during the subsequent winter to the total number of warm (cold) PMM events. Through mathematical deviations (see Text S1 in Supporting Information S1), we illustrate that the efficacy of warm or cold PMMs can be dissected into contributions from three distinct origin groups (El Niño-induced, La Niña-induced, and internal atmosphere-induced) of PMM events. The proportionate impact of each group on the overall efficacy is determined by multiplying the sub-efficacy of each origin group by the percentage of warm or cold

PMMs attributed to that group. Both total efficacy and sub-efficacy are expressed as values ranging from 0.0 to 1.0, while the percentage spans from 0.0% to 100.0%.

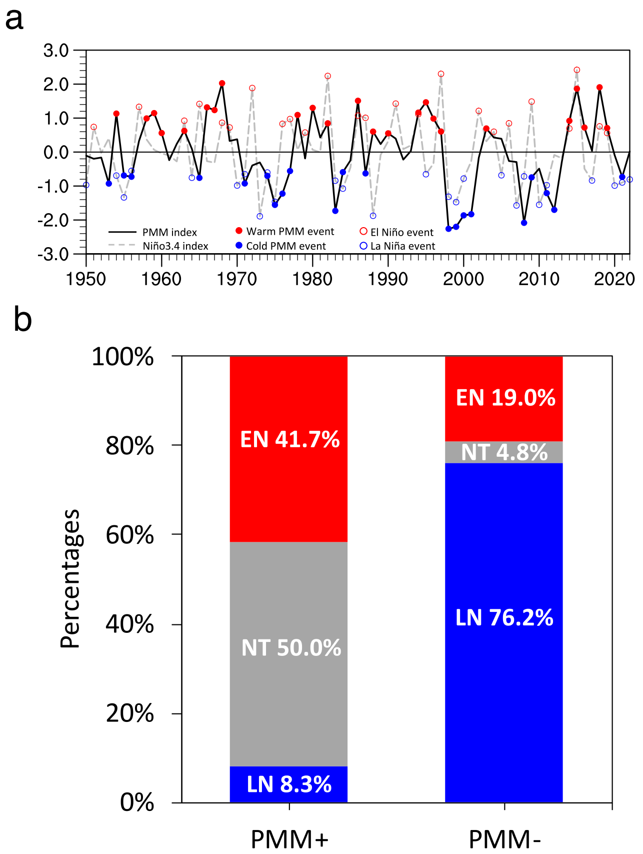

Figure 1. (a) Time series of boreal spring (MAM^0) PMM index (solid-black line) and the following winter (ND^{0}J^1) Niño3.4 index (dash-gray line). Solid red (blue) circles indicate warm (cold) PMM events, while hollow red (blue) circles represent El Niño (La Niña) events. (b) Percentages of warm and cold PMM events preceded by El Niño (EN; red bar), Neutral (NT; gray bar), and La Niña (LN; blue bar) conditions in the previous winter (ND^{-1} J^0).

3. Results

3.1. Asymmetric Efficacies Between Warm and Cold PMMs and Linkages to Their Asymmetric Origins and Sub-Efficacies

Figure 1a illustrates the time series of the boreal spring (MAM^0) PMM index alongside the subsequent winter (ND^{0}J^1) Niño3.4 index. In this study, the superscript "0" denotes the developing year of the PMM, the superscript "1" represents the following year, and the superscript "–1" represents the previous year. Overall, a noticeable tendency exists for the PMM and Niño3.4 indices to co-vary. Their positive linear correlation (R = 0.37) proves statistically significant at a 99% confidence level, aligning with the prior research that the PMM acts as a precursor to ENSO occurring several months later (Chang et al., 2007; Larson & Kirtman, 2014). Analyzing 24 warm PMMs and 21 cold PMM events spanning 1950–2022, we observed that 13 out of the 21 cold PMM events were succeeded by a La Niña, outnumbering the 10 out of 24 warm PMM events that led to an El Niño. This underscores a 0.62 efficacy for cold PMM in linking to subsequent La Niña, contrasting with a 0.42 efficacy for warm PMM in linking to subsequent El Niño, thereby exposing a significant asymmetry between the efficacies of warm and cold PMMs. To validate this finding, we utilized alternative indices, namely the PMM Wind index and the PMM area-averaged index, to re-identify warm and cold PMM events. The recalculated efficacies for both alternative PMM indices consistently showed a robust higher efficacy for cold PMM in inducing La Niña (0.68 vs. 0.54 and 0.65 vs. 0.40; see Figures S1 and S2 in Supporting Information S1) compared to warm PMM inducing El Niño.

We find that the asymmetric efficacies between warm and cold PMMs stem from two sources: the differing origins of these PMMs and the varying sub-efficacies associated with each origin group. To demonstrate the first source, we categorized the 24 warm and 21 cold PMM events into three groups based on their origins (Table S1 in Supporting Information S1 and Figure 1b). These groups are delineated by the ENSO conditions in the preceding winter (ND^{-1} J^0) of the PMM. Specifically, we identified PMM events preceded by El Niño ("EN") as EN-induced, those preceded by La Niña ("LN") as LN-induced, and those occurring under ENSO neutral condition ("NT") as NT-induced. Our classification reveals that warm PMM events are comparably activated by both El Niño (10 cases, 41.7%) and atmospheric internal dynamics (12 cases, 50.0%), with only a minor proportion induced by La Niña (2 cases, 8.3%). In contrast, cold PMM events predominantly belong to the LN-induced group (16 cases, 76.2%), followed by the EN-induced group (4 cases, 19.0%), and a minimal fraction associated with the internal dynamics group (1 case, 4.8%).

Fang and Yu (2020a) have already explained why El Niño and La Niña can activate PMM events. They suggested that CP ENSO in the tropical central Pacific play a key role in activating corresponding phases of PMM events. During a CP El Niño (La Niña), anomalous heating (cooling) in the tropical central Pacific induces a Gill-type atmospheric response, resulting in abnormal southwesterly (northeasterly) winds over the extratropical North Pacific. These anomalous winds, in turn, trigger a warm (cold) phase of the PMM. Fang and Yu (2020a) also suggested that ENSO in the tropical eastern Pacific (i.e., the EP ENSO) can activate an out-of-phase PMM. An EP El Niño activates a cold phase of the PMM, in contrast to the warm PMM activated by a CP El Niño. This distinction arises from the further eastward location of the anomalous heating induced by the EP El Niño. Consequently, its Gill response in the atmosphere produces anomalous northeasterly winds over the extratropical North Pacific, leading to the activation of a cold PMM. Conversely, the La Niña over the tropical eastern Pacific can activate a warm PMM. Consistent with Fang and Yu (2020a), we observed that the El Niño preceding the warm PMM (Figure 2a) and the La Niña preceding the cold PMM (Figure 2b) both exhibit a composite SSTA

10.1029/2024GL108924

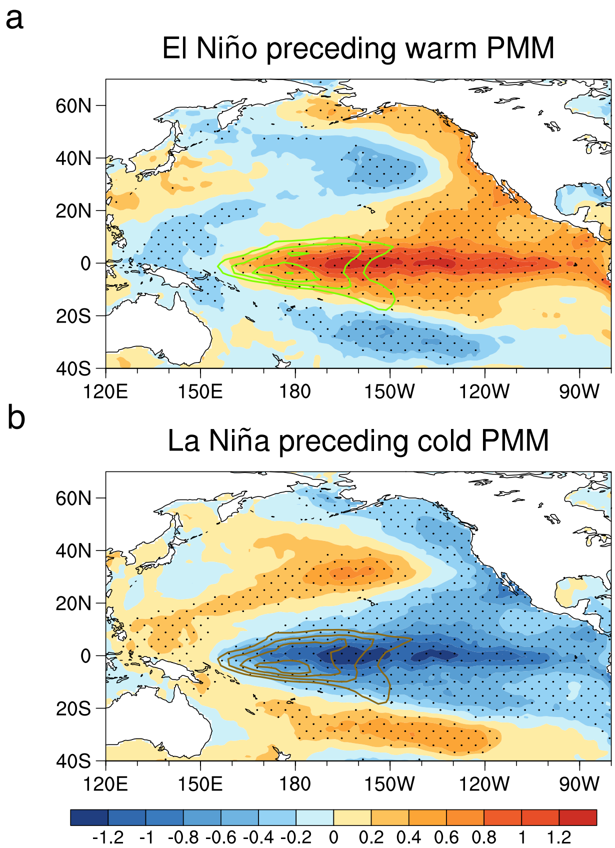

Figure 2. Composite SSTAs (shading; °C) and precipitation anomalies (contour; green lines for positive values and brown lines for negative values, each with a 1 mm/day interval) during (a) the El Niño events that induce warm PMM events and during (b) the La Niña events that induce cold PMM events. Dots represent the SSTAs that are significant at a 95% confidence level.

pattern resembling the CP ENSO, with the SSTA center west of 150°W. The composite SSTAs are concentrated in the tropical central Pacific, extending northeastward toward Baja California (Figure 2; Kao & Yu, 2009). In contrast, the El Niño preceding the cold PMM (Figure S3a in Supporting Information S1) and the La Niña preceding the warm PMM (Figure S3b in Supporting Information S1) both exhibit a composite SSTA pattern reminiscent of the EP ENSO, characterized by significant SSTAs spanning from the tropical eastern Pacific to the tropical central Pacific.

Why does the cold PMM exhibit a notably higher proportion of the LN-induced origin group compared to the warm PMM's proportion of the EN-induced origin group? There are two potential explanations. First, La Niña tend to be predominantly of the CP type, whereas El Niño were primarily of the EP type in the 20th century but have shifted to a predominance of the CP type since the 1990s (Capotondi et al., 2015; Chen et al., 2019; Li et al., 2024). This higher frequency of CP La Niña compared to CP El Niño during our analysis period serves as the first potential explanation for the asymmetric origins between the warm and cold PMMs. Second, CP La Niña and CP El Niño exhibit differential effectiveness in activating the cold and warm PMMs. Fang and Yu (2020a) demonstrated that CP La Niña can induce a stronger atmospheric Gill response, effectively triggering the cold PMM. Conversely, CP El Niño are less effective in eliciting the necessary Gill response to activate the warm PMMs. This disparity arises from the tropical central Pacific having a background mean SST value close to and slightly above the threshold SST value for deep convection (about 28°C). The cooling associated with a La Niña can drop the local SST below this threshold to shut down the deep convection, resulting in an anomalous cooling much larger than the anomalous heating produced by the warming associated with a comparable intensity of El Niño. Their suggestion is supported by the composite precipitation anomalies for the EN-induced warm PMM and LN-induced cold PMM groups (Figure 2). In the figure, the negative precipitation anomalies over the tropical central Pacific in the LN-induced group of cold PMM are stronger than the positive precipitation anomalies in the EN-induced warm PMM group.

We now focus on the second source explaining the asymmetric efficacies between warm and cold PMMs in inducing ENSOs. As mentioned earlier, this source is related to the varying sub-efficacies associated with the origin groups of warm and cold PMMs. As detailed in Section 2.2, the efficacy of warm or cold PMMs is determined by the cumulative sub-efficacy of each of their three origin groups, weighted by the percentage of that group in the total number of warm or cold PMMs. The sub-efficacy is calculated as the ratio of warm (cold) PMM events in each origin group followed by an El Niño (La Niña) in the subsequent winter. Figure 3a reveals that while warm PMM consists of EN-induced and NT-induced groups in comparable proportions (41.7% and 50.0%), the EN-induced group exhibits an unusually low sub-efficacy (0.20) in inducing El Niño compared to the higher sub-efficacy of the NT-induced group (0.50). The diminished sub-efficacy observed in the EN-induced PMM group constitutes the primary factor contributing to the overall lower efficacy of warm PMM. As depicted in Figure 3c, despite constituting 41.7% of warm PMM events, the EN-induced group contributes only 0.08 to the total efficacy of 0.42. The LN-induced group, while having a sub-efficacy (0.50) comparable to the NT-induced group (0.58), constitutes only a minor percentage (8.3%) of warm PMMs and does not significantly impact the total efficacy of warm PMM. For cold PMM (Figure 3b), the dominant LN-induced group (76.2%) exhibits a sub-efficacy of 0.69. The remarkably high sub-efficacy and its strong dominance in the LN-induced group are the primary contributors to the overall higher efficacy of cold PMMs. This group contributes 0.52 to the total efficacy of 0.62 for cold PMMs (Figure 3d), while the contributions from the other two origin groups are minimal.

In summary, the significant asymmetry between the higher efficacy of cold PMM in inducing La Niña and the lower efficacy of warm PMM in inducing El Niño can be attributed primarily to the unusually low sub-efficacy of EN-induced warm PMM events and the abnormally high sub-efficacy of LN-induced cold PMM events. The

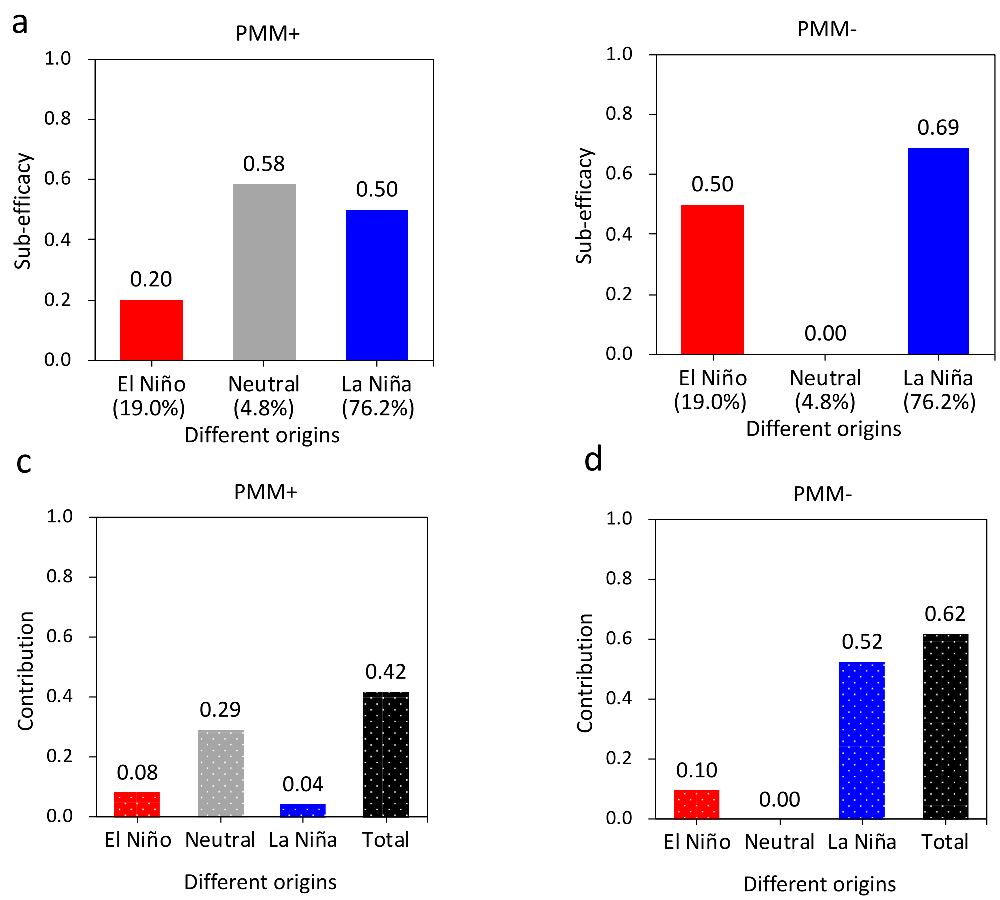

Figure 3. (a) Sub-efficacies of the three groups of warm PMM (i.e., the EN-induced group, NT-induced group, and LN-induced group) in triggering subsequent El Niño. Panel (b) same as (a), but for the three groups of cold PMM in triggering La Niña. Black numbers on the top of the bars represent the sub-efficacy of each group, while the numbers on the *x*-axis labels are the percentage of that group in accounting for the total number of warm or cold PMM events (same as those shown in Figure 1b). (c) Respective contributions of each group to the total efficacy of warm PMM, calculated by multiplying their sub-efficacies and the number percentages. (d) Same as (c), but for cold PMM. In (a)–(d), the *x*-axis always represents different groups, with "El Niño" representing the EN-induced group, "Neutral" representing the NT-induced group, and "La Niña" representing the LN-induced group.

cause for the different sub-efficacies between these two PMM groups is related to the varying competitions among these PMMs, with the discharged-recharged states left over from the preceding El Niño and La Niña events that activated the PMMs. We demonstrate this competition in detail in the next section.

3.2. Competition of PMM With Tropical Discharge-Recharge Processes

The discharge (recharge) process linked to El Niño (La Niña) typically depletes (accumulates) OHC in the tropical Pacific, favoring the development of the opposite condition in the following year. Both EN- and LN-induced PMM events must contend with the residual discharge/recharge states from preceding ENSO events to influence the likelihood of triggering an ENSO event in the subsequent winter. Examining the changes in SST, 850 hPa wind, and upper-300 m OHC anomalies from the year preceding the PMM to the PMM year across these two groups of PMM events reveals contrasting discharge-recharge patterns (Figures S4 and S5 in Supporting Information S1). Specifically, the OHC anomalies shift to a negative phase for EN-induced warm PMM in MAM^0, indicating discharge from the preceding El Niño, while they remain negative for LN-induced cold PMM. This OHC asymmetry is clearer when summing the composite OHC anomalies between these PMM groups along the equatorial Pacific (5°S–5°N) during MAM^0 (Figure 4). The overall negative summation suggests a stronger OHC discharge from the preceding El Niño for EN-induced warm PMM compared to the OHC recharge from the preceding La Niña for LN-induced cold PMM. The EN-induced warm PMM has to compete with stronger

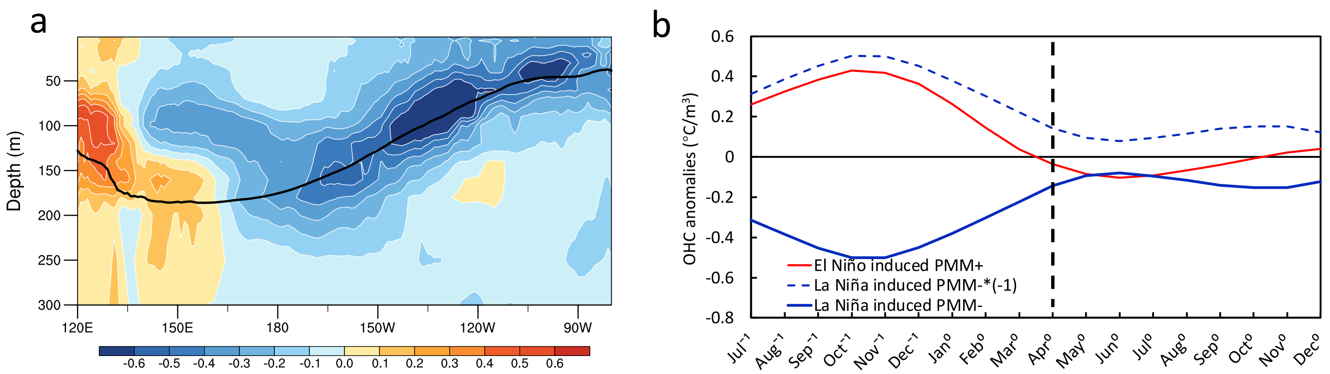

Figure 4. (a) Summation of the composite ocean temperature anomalies of EN-induced warm PMM and LN-induced cold PMM along the equatorial (5°S–5°N) Pacific during MAM^0. Black line indicates the climatology thermocline depth (represented by the depth of the 20°C isotherm). (b) Composite evolution of mean OHC anomalies (horizontally averaged between 5°S–5°N and 120°E–80°W and vertically averaged from 0 to 300 m) from the preceding year to the developing year of the EN-induced warm PMM (red solid line) and LN-induced cold PMM (blue solid line). For comparison, the evolution of LN-induced cold PMM is multiplied by −1 and replicated as a blue dashed line. Vertical black dashed line indicate the MAM^0 season.

discharged OHC to induce El Niño, while the LN-induced cold PMM faces weaker competition to induce La Niña. Consequently, LN-induced cold PMM is more effective in inducing La Niña (see Figures S5e–S5h in Supporting Information S1), whereas EN-induced warm PMM faces challenges inducing El Niño due to competition from stronger discharged OHC (see Figures S4e–S4h in Supporting Information S1). This asymmetric strength in OHC anomalies is a key reason why the LN-induced cold PMM is more capable of inducing La Niña than the EN-induced warm PMM in inducing El Niño.

Why does the El Niño preceding the warm PMM result in a stronger discharge of the OHC state than the recharge OHC state produced by the La Niña preceding the cold PMM? To answer this question, we compared the evolution of mean OHC anomalies between these two PMM groups in Figure 4b. These anomalies are horizontally averaged between 5°S–5°N and 120°E–80°W and vertically averaged from 0 to 300 m. Consistent with Figure 4a, we observed that during the MAM^0 season, the mean OHC state for the EN-induced warm PMM has already been depleted to a negative anomaly (−0.03°C), while the OHC state in the LN-induced cold PMM group remains strongly negative (−0.14°C) (Figure 4b). Both groups exhibit peaked mean OHC anomalies in the preceding October. Subsequently, the El Niño group discharged rapidly toward MAM^0, wiping out the peak positive OHC anomalies, whereas the recharging of the La Niña proceeded slowly toward the MAM^0 season, leaving the OHC still negative. Previous studies have already noted this asymmetric discharge/recharge feature between El Niño and La Niña, attributing it to factors such as stronger typical El Niño intensities compared to La Niña (Burgers & Stephenson, 1999; Deser & Wallace, 1987; Jin et al., 2003), the more eastward location of El Niño compared to La Niña (Okumura & Deser, 2010), and their different meridional widths (Hu et al., 2017).

Another factor that also contributes to the asymmetric efficacies of the EN-induced warm PMM and LN-induced cold PMM is their different intensities. LN-induced cold PMM tends to be stronger, with a mean value of −1.22 standard deviations compared to 1.08 standard deviations for EN-induced warm PMM. This intensity asymmetry allows LN-induced cold PMM to exert a greater impact on the tropical Pacific, leading to uneven efficacy between the two types of ENSO-induced PMM events. This observation aligns with previous research by Fan et al. (2023a, 2023b), which identified a negative skewness between ENSO-induced cold and warm phases of PMM events.

4. Summary and Discussion

This study discovered that cold PMM is more effective in triggering La Niña, contrary to previous beliefs favoring warm PMM's influence on El Niño. This efficacy asymmetry stems from differences in sub-efficacies within ENSO-induced PMM groups rather than those generated by atmospheric internal dynamics. Specifically, the disparity is most pronounced between EN-induced warm PMM and LN-induced cold PMM, with the former showing low sub-efficacy and the latter exhibiting high sub-efficacy. This discrepancy is mainly due to EN-induced weak warm PMM contending with a stronger discharged OHC state in the equatorial Pacific following the preceding El Niño, while the competitive effect is weaker for strong cold PMM, enabling it to generate subsequent La Niña more efficiently. Our study highlights the significance of comprehending not just the phase of the PMM, but also its origin in the context of ENSO research and prediction (Zheng & Yu, 2017).

Our findings also provide a new explanation for why La Niña has a higher tendency for multi-year or prolonged events than El Niño (Gao et al., 2023; Okumura & Deser, 2010). Previous studies have associated the El Niño-La Niña asymmetric evolution with factors such as the nonlinearity of atmospheric processes (Hoerling et al., 1997), the asymmetric impact of the Indian Ocean (Okumura & Deser, 2010), and oceanic wave mechanisms linked to asymmetric recharge and discharge processes (Hu et al., 2014). Our study suggests that the asymmetric efficacies between warm and cold PMMs represent another crucial process in ENSO asymmetric evolution. La Niña events are more adept at triggering the cold phase of PMM after the La Niña peaks. The La Niña-induced cold PMM is then more efficient at triggering the following year's La Niña, contributing to the generation of more multi-year La Niña. While similar processes may occur during El Niño, the El Niño-induced warm PMM has a lower efficacy in generating subsequent El Niño events, resulting in fewer multi-year El Niño.

Our findings also support Kim et al. (2023)'s assertion that PMM plays a pivotal role in elucidating multi-year La Niña events. We found that only 12 out of 26 (0.46; Table S2 in Supporting Information S1) instances of first-year La Niña were followed by a second-year La Niña. However, when the first-year La Niña triggers a cold PMM event, the likelihood of a second-year La Niña rises to 0.69 (11 out of 16 cases; Table S2 in Supporting Information S1). Conversely, if the first-year La Niña fails to activate a cold PMM event, there is a high probability (0.9) that a second-year La Niña will not occur (9 out of 10 cases; Table S2 in Supporting Information S1).

Data Availability Statement

In this study, monthly SST data were sourced from the Hadley Center Sea Ice and SST data set (Rayner et al., 2003). Monthly 850 hPa wind data originated from the National Centers for Environmental Prediction/National Center for Atmospheric Research Reanalysis 1 (Kalnay et al., 1996). Monthly subsurface temperature data were obtained from the Institute of Atmospheric Physics global ocean temperature gridded product with a $1° \times 1°$ horizontal resolution (Cheng et al., 2017). Monthly precipitation data was taken from the National Oceanic and Atmospheric Administration's Precipitation Reconstruction (Chen et al., 2004). The PMM SST and Wind indices are sourced from the University of Wisconsin–madison (Chiang & Vimont, 2004). The analysis encompasses the period from 1950 to 2022. Anomalies are determined as the deviations from the seasonal cycle, computed as the average over the analysis period, subsequent to the removal of linear trends.

Acknowledgments
This research was supported by the Climate and Large-Scale Dynamics Program of the U. S. National Science Foundation under Grants AGS-2109539. The authors express their gratitude to Editor Suzana Camargo and two anonymous reviewers for their invaluable feedback, which significantly contributed to enhancing the quality of the article.

References

Anderson, B. T., Perez, R. C., & Karspeck, A. (2013). Triggering of El Niño onset through trade wind–induced charging of the equatorial Pacific. *Geophysical Research Letters*, *40*(6), 1212–1216. https://doi.org/10.1002/grl.50200

Burgers, G., & Stephenson, D. B. (1999). The "normality" of El Niño. *Geophysical Research Letters*, *26*(8), 1027–1030. https://doi.org/10.1029/1999GL900161

Capotondi, A., Wittenberg, A. T., Newman, M., Lorenzo, E. D., Yu, J.-Y., Braconnot, P., et al. (2015). Understanding ENSO diversity. *Bulletin of the American Meteorological Society*, *96*(6), 921–938. https://doi.org/10.1175/BAMS-D-13-00117.1

Chang, P., Zhang, L., Saravanan, R., Vimont, D. J., Chiang, J. C. H., Ji, L., et al. (2007). Pacific meridional mode and El Niño—Southern Oscillation. *Geophysical Research Letters*, *34*(16),L16608. https://doi.org/10.1029/2007GL030302

Chen, M., Xie, P., Janowiak, J. E., Arkin, P. A., & Smith, T. M. (2004). Verifying the reanalysis and climate models outputs using a 56-year data set of reconstructed global precipitation [Dataset]. *14th AMS Conf. Appl. Meteor*. Retrieved from https://psl.noaa.gov/data/gridded/data.prec.html

Chen, M., Yu, J.-Y., Wang, X., & Jiang, W. (2019). The changing impact mechanisms of a diverse El Niño on the Western Pacific subtropical high. *Geophysical Research Letters*, *46*(2), 953–962. https://doi.org/10.1029/2018GL081131

Cheng, L., Trenberth, K. E., Fasullo, J., Boyer, T., Abraham, J., & Zhu, J. (2017). Improved estimates of ocean heat content from 1960 to 2015 [Dataset]. *Science Advances*, *3*(3), e1601545. https://doi.org/10.1126/sciadv.1601545

Chiang, J. C. H., & Vimont, D. J. (2004). Analogous Pacific and Atlantic meridional modes of tropical atmosphere–ocean variability [Dataset]. *Journal of Climate*, *17*(21), 4143–4158. https://doi.org/10.1175/jcli4953.1

Deser, C., & Wallace, J. M. (1987). El Niño events and their relation to the Southern Oscillation: 1925–1986. *Journal of Geophysical Research*, *92*(C13), 14189–14196. https://doi.org/10.1029/JC092iC13p14189

Ding, R., Tseng, Y.-H., Di Lorenzo, E., Shi, L., Li, J., Yu, J.-Y., et al. (2022). Multi-year El Niño events tied to the North Pacific Oscillation. *Nature Communications*, *13*(1), 3871. https://doi.org/10.1038/s41467-022-31516-9

Fan, H., Huang, B., Yang, S., & Dong, W. (2021). Influence of the Pacific meridional mode on ENSO Evolution and Predictability: Asymmetric modulation and ocean preconditioning. *Journal of Climate*, *34*(5), 1881–1901. https://doi.org/10.1175/JCLI-D-20-0109.1

Fan, H., Wang, C., & Yang, S. (2023a). Asymmetry between positive and negative phases of the Pacific meridional mode: A contributor to ENSO transition complexity. *Geophysical Research Letters*, *50*(14), e2023GL104000. https://doi.org/10.1029/2023GL104000

Fan, H., Yang, S., Wang, C., & Lin, S. (2023b). Revisiting the impacts of tropical Pacific SST anomalies on the Pacific meridional mode during the decay of strong eastern Pacific El Niño events. *Journal of Climate*, *36*(15), 4987–5002. https://doi.org/10.1175/JCLI-D-22-0342.1

Fang, S., & Yu, J. (2020a). A control of ENSO transition complexity by tropical Pacific mean SSTs through tropical-subtropical interaction. *Geophysical Research Letters*, *47*(12), e2020GL087933. https://doi.org/10.1029/2020GL087933

Fang, S., & Yu, J. (2020b). Contrasting transition complexity between El Niño and La Niña: Observations and CMIP5/6 models. *Geophysical Research Letters*, *47*(16), e2020GL088926. https://doi.org/10.1029/2020GL088926

Gao, Z., Hu, Z.-Z., Zheng, F., Li, X., Li, S., & Zhang, B. (2023). Single-year and double-year El Niños. *Climate Dynamics*, *60*(7), 2235–2243. https://doi.org/10.1007/s00382-022-06425-8

Hoerling, M. P., Kumar, A., & Zhong, M. (1997). El Niño, La Niña, and the nonlinearity of their teleconnections. *Journal of Climate*, *10*(8), 1769–1786. https://doi.org/10.1175/1520-0442(1997)010<1769:ENOLNA>2.0.CO;2

Hu, Z.-Z., Kumar, A., Huang, B., Zhu, J., Zhang, R.-H., & Jin, F.-F. (2017). Asymmetric evolution of El Niño and La Niña: The recharge/discharge processes and role of the off-equatorial sea surface height anomaly. *Climate Dynamics*, *49*(7), 2737–2748. https://doi.org/10.1007/s00382-016-3498-4

Hu, Z.-Z., Kumar, A., Xue, Y., & Jha, B. (2014). Why were some La Niñas followed by another La Niña? *Climate Dynamics*, *42*(3), 1029–1042. https://doi.org/10.1007/s00382-013-1917-3

Jin, F.-F. (1997). An equatorial ocean recharge paradigm for ENSO. Part I: Conceptual model. *Journal of the Atmospheric Sciences*, *54*(7), 811–829. https://doi.org/10.1175/1520-0469(1997)054<0811:AEORPF>2.0.CO;2

Jin, F.-F., An, S.-I., Timmermann, A., & Zhao, J. (2003). Strong El Niño events and nonlinear dynamical heating. *Geophysical Research Letters*, *30*(3), 1120. https://doi.org/10.1029/2002GL016356

Kalnay, E., Kanamitsu, M., Kistler, R., Collins, W., Deaven, D., Gandin, L., et al. (1996). The NCEP/NCAR 40-year reanalysis project [Dataset]. *Bulletin of the American Meteorological Society*, *77*(3), 437–472. https://doi.org/10.1175/1520-0477(1996)077<0437:TNYRP>2.0.CO;2

Kao, H.-Y., & Yu, J.-Y. (2009). Contrasting eastern-Pacific and central-pacific types of ENSO. *Journal of Climate*, *22*(3), 615–632. https://doi.org/10.1175/2008JCLI2309.1

Kim, J.-W., Yu, J.-Y., & Tian, B. (2023). Overemphasized role of preceding strong El Niño in generating multi-year La Niña events. *Nature Communications*, *14*(1), 6790. https://doi.org/10.1038/s41467-023-42373-5

Larson, S. M., & Kirtman, B. P. (2014). The Pacific meridional mode as an ENSO precursor and predictor in the North American multimodel ensemble. *Journal of Climate*, *27*(18), 7018–7032. https://doi.org/10.1175/JCLI-D-14-00055.1

Li, X., Yu, J.-Y., & Ding, R. (2024). El Niño-La Niña asymmetries in the changes of ENSO complexities and dynamics since 1990. *Geophysical Research Letters*, *51*(6), e2023GL106395. https://doi.org/10.1029/2023GL106395

Meng, Z., & Li, T. (2023). Why is the Pacific meridional mode most pronounced in boreal spring? *Climate Dynamics*, *62*(1), 459–471. https://doi.org/10.1007/s00382-023-06914-4

Okumura, Y. M., & Deser, C. (2010). Asymmetry in the duration of El Niño and La Niña. *Journal of Climate*, *23*(21), 5826–5843. https://doi.org/10.1175/2010JCLI3592.1

Rayner, N. A. A., Parker, D. E., Horton, E. B., Folland, C. K., Alexander, L. V., Rowell, D. P., et al. (2003). Global analyses of sea surface temperature, sea ice, and night marine air temperature since the late nineteenth century [Dataset]. *Journal of Geophysical Research*, *108*(D14), 4407. https://doi.org/10.1029/2002JD002670

Richter, I., Stuecker, M. F., Takahashi, N., & Schneider, N. (2022). Disentangling the North Pacific meridional mode from tropical Pacific variability. *Npj Climate and Atmospheric Science*, *5*(1), 1–9. https://doi.org/10.1038/s41612-022-00317-8

Thomas, E. E., & Vimont, D. J. (2016). Modeling the mechanisms of linear and nonlinear ENSO responses to the Pacific meridional mode. *Journal of Climate*, *29*(24), 8745–8761. https://doi.org/10.1175/JCLI-D-16-0090.1

Vimont, D. J., Battisti, D. S., & Hirst, A. C. (2001). Footprinting: A seasonal connection between the tropics and mid-latitudes. *Geophysical Research Letters*, *28*(20), 3923–3926. https://doi.org/10.1029/2001GL013435

Vimont, D. J., Wallace, J. M., & Battisti, D. S. (2003). The seasonal footprinting mechanism in the Pacific: Implications for ENSO. *Journal of Climate*, *16*(16), 2668–2675. https://doi.org/10.1175/1520-0442(2003)016<2668:TSFMIT>2.0.CO;2

Wang, C., Deser, C., Yu, J.-Y., DiNezio, P., & Clement, A. (2017). El Niño and Southern Oscillation (ENSO): A review. In P. W. Glynn, D. P. Manzello, & I. C. Enochs (Eds.), *Coral reefs of the eastern tropical Pacific: Persistence and loss in a dynamic environment* (pp. 85–106). Springer Netherlands. https://doi.org/10.1007/978-94-017-7499-4_4

Xie, S., & Philander, S. G. H. (1994). A coupled ocean-atmosphere model of relevance to the ITCZ in the eastern Pacific. *Tellus*, *46*(4), 340–350. https://doi.org/10.1034/j.1600-0870.1994.t01-1-00001.x

Yang, S., Li, Z., Yu, J.-Y., Hu, X., Dong, W., & He, S. (2018). El Niño–Southern Oscillation and its impact in the changing climate. *National Science Review*, *5*(6), 840–857. https://doi.org/10.1093/nsr/nwy046

Yu, J.-Y., Kao, H.-Y., & Lee, T. (2010). Subtropics-related interannual sea surface temperature variability in the central equatorial Pacific. *Journal of Climate*, *23*(11), 2869–2884. https://doi.org/10.1175/2010JCLI3171.1

Yu, J.-Y., & Kim, S. T. (2011). Relationships between extratropical sea level pressure variations and the central Pacific and eastern Pacific types of ENSO. *Journal of Climate*, *24*(3), 708–720. https://doi.org/10.1175/2010JCLI3688.1

Zheng, F., & Yu, J.-Y. (2017). Contrasting the skills and biases of deterministic predictions for the two types of El Niño. *Advances in Atmospheric Sciences*, *34*(12), 1395–1403. https://doi.org/10.1007/s00376-017-6324-y

Zheng, Y., Chen, W., Chen, S., Yao, S., & Cheng, C. (2021). Asymmetric impact of the boreal spring Pacific meridional mode on the following winter El Niño-Southern Oscillation. *International Journal of Climatology*, *41*(6), 3523–3538. https://doi.org/10.1002/joc.7033